

Gaussian-Middleton Classification of Cyclostationary Correlated Noise in Hybrid MIMO-OFDM WiNPLC

Sadaf Moaveninejad*, Atul Kumar[§], Mahmoud Elgenedy[†], Maurizio Magarini*, Naofal Al-Dhahir[†], and Andrea M. Tonello[‡]

*Department of Electronic, Information and Bioengineering, Politecnico di Milano, Milano, Italy
Email: {sadaf.moaveninejad, and maurizio.magarini}@polimi.it.

[§] Vodafone Chair Mobile Communications Systems, Technische Universität Dresden, Germany.
Email: atul.kumar@tu-dresden.de.

[†]Department of Electrical and Computer Engineering, University of Texas at Dallas, Tx USA
Email: {mahmoud.elgenedy, aldhahir}@utdallas.edu.

[‡]Chair of Embedded Communication Systems, University of Klagenfurt 9020 Klagenfurt, Austria
Email: andrea.tonello@aau.at.

Abstract—An effective approach to enhance the data rate in narrowband power line communication (NBPLC) system is multi-carrier modulation based on orthogonal frequency-division multiplexing (OFDM) and multiple-input multiple-output (MIMO) transmission over multiple power line phases. A key challenge for achieving reliable communication over MIMO-OFDM NBPLC is to mitigate the effects of the correlated non-stationary additive noise. In fact, substantial components of the noise in NBPLC systems exhibit a cyclostationary behavior with a period of half the AC cycle. Moreover, when MIMO transmission is adopted, an important issue that must be considered is the cross-correlation between the different phases. In this work, we propose to classify the cyclostationary noise into three classes, based on the evaluation of second order statistics. In addition, we derive estimates of the probability density functions for each of the three classes and show that while two of them exhibit a Gaussian behavior, the third one has an impulsive behaviour similar to the Middleton class-A noise. Simulation results show that the bit error rate (BER) of MIMO-OFDM NBPLC significantly changes between different classes of noise. Hence, we develop an algorithm for switching data delivery between MIMO-OFDM NBPLC and MIMO-OFDM wireless transmission in unlicensed frequency band that takes into account knowledge of the periodicity of the three classes of noises. The result is a hybrid MIMO-OFDM wireless/NBPLC system, which we refer to as, hybrid MIMO-OFDM WiNPLC. Our simulation results demonstrate BER improvement of the proposed hybrid system over individual MIMO-OFDM NBPLC or MIMO-OFDM wireless systems.

Index Terms—Powerline communication (PLC), Noise Classification, Cyclostationary Noise, Correlated Noise, Hybrid wireless-PLC, WiNPLC, Narrowband PLC, OFDM, MIMO, Smart grids.

I. INTRODUCTION

Narrowband power line communications (NBPLC) has been receiving increased popularity recently as a strong candidate to connect meters with local utilities, thus enabling intelligent monitoring and control of energy flows in the electric network [1], [2]. This is the first path for transition from a conventional power network towards smart grids (SG).

Narrowband communication over power line was initially proposed for single-carrier modulation and single-input single-output (SISO) transmission. NBPLC operates in the frequency range between 3kHz and 500 kHz and provides low data rates on the order of few kilo bits per second (kbps). Higher data rates (HDR) up to 800 kbps are obtained by introducing orthogonal frequency-division multiplexing (OFDM), which mitigates inter-symbol interference (ISI) introduced by the frequency-selectivity of the channel [3]. HDR is required for new applications in SG, for improving the efficiency of tele-management services, and for decreasing the time to access a meter's data. To achieve further enhancements in the data rate of NBPLC, the combination of OFDM and multiple-input multiple-output (MIMO) transmission is considered an attractive solution. Other advantages of MIMO include not requiring high transmission power or large bandwidth [4]. Implementing MIMO-OFDM allows the limited bandwidth of NBPLC to be employed more efficiently and with higher reliability. In addition to HDR, establishing communication services in SG also requires high reliability.

Two fundamental challenges must be overcome to achieve reliable transmission in MIMO-OFDM NBPLC: i) impairments due to time-varying noise [5]–[7]; ii) cross-correlation of the noises affecting multiple phases [4]. Impulsive non-Gaussian additive noise, as the other major impairment in NBPLC, requires precise modeling and analysis of its statistics. Although in many earlier works authors simply considered it to be additive white Gaussian noise (AWGN), in practice, it is given by the superposition of different noise sources [3]. In addition, noise in NBPLC has periodic temporal and spectral properties that are synchronous to AC mains cycle [5], [6]. Moreover, in MIMO channels, the cross-correlation between the different phases must also be taken into account in the noise modeling. A model for the correlated cyclostationary noise for MIMO NBPLC, based on the use of frequency shift

(FRESH) filtering, is given in [4], which was validated by comparison with real measurements.

In addition to considering the aforementioned methodological implementation of MIMO NBPLC based on OFDM modulation, which includes also the cyclostationary correlated noise, this paper has three main contributions. First, it analyzes the cyclostationary noise and show that it can be statistically classified into three different classes per each cycle. To the best of the authors knowledge, this is the first work that classifies cyclostationary noise in MIMO NBPLC based on its statistics. The idea of statistical classification proposed in this work is more generic and accurate than temporal region classification proposed in [3], [5], [8] since it does not restrict the classes to be continuous in time. Specifically, authors in [5] modeled the cyclostationary noise as three temporal regions stationary colored noise, where each noise temporal region is assumed to have a Gaussian distribution with different power spectral densities. However, the number of regions and the regions boundaries were determined based on visual inspection. In [9], the authors a priori assumed three temporal regions similar to [5], and proposed to detect the temporal regions boundaries using a double-sliding energy window. A novel aspect of this work is to analyze the distributions of the noise samples of each class and compare each of them with a normal distribution. Such analysis reveals that the pdf of two classes fit a Gaussian distribution but the third one is more impulsive and non-Gaussian, which was not considered by [3], [5], [8]. As the second contribution of this paper, the performance of the MIMO-OFDM NBPLC system during each of the three noise classes is compared with that of a wireless link in terms of bit error rate (BER) versus signal-to-noise ratio (SNR). Finally, the third contribution is an algorithm for switching between MIMO-OFDM wireless and MIMO-OFDM NBPLC over the different classes of noise, which is referred to as a hybrid MIMO-OFDM wireless/NBPLC (WiNPLC) communication system. The proposed hybrid system takes advantage of the independence of the noise and of the channel characteristics of wireless and powerline links to improve the transmission reliability in smart grids. It is demonstrated that the hybrid system enhances reliability and coverage [10]–[12]. The authors in [13] investigated the advantages of using cooperative transmission in a hybrid scheme from both technical and infrastructural perspectives. There are very few investigations on simultaneous transmission in a hybrid wireless/PLC systems. To the best knowledge of the authors, previous works were based on simultaneous transmission over wireless/PLC with receive diversity combining [10], [11], [14]. However in this work, we proposed a switching algorithm based on the temporal behaviour of the noise in NBPLC and average received SNR in each period. Considering the cyclic behaviour of the noise, the same algorithm can be followed in next periods as long as the average received SNR is the same. An important advantage of our proposed hybrid system over previous works is that switching is done using only the average SNR corresponds to the received data in one period of the cyclostationary noise, not the SNR per sub-channel or per

OFDM symbol. Switching or combining based on the SNR per sub-channel, means that, for each OFDM symbol, it requires computing the whole noise power spectral densities (PSD) as done in [15]. However, in our case, we calculate only a single number which is the average noise variance, and this is interesting from a practical point of view since it has a very low complexity.

Hereinafter, MIMO-OFDM NBPLC and MIMO-OFDM wireless links in our system are referred to as NBPLC and wireless, respectively.

The rest of this paper is organized as follows. In Sec. II, we present background on MIMO FRESH filter noise modeling. The system model is presented in Sec. III, while the configuration of the hybrid WiNPLC system is presented in Sec. IV. Section V describes our approach for classification of noise to different temporal regions inside each cycle. Simulation results and switching strategies are presented in Sec. VI. Finally, conclusion and future works are discussed in Sec. VII.

II. CYCLOSTATIONARY NOISE MODELING IN MIMO NBPLC

NBPLC noise consists of the superposition of different components. In addition to AWGN term, the other components are usually characterized by statistical properties with a periodicity that is synchronous with AC mains cycle [6]. In particular, impulsive noise is characterized by an amplitude pdf that is non-Gaussian. The authors of [5] and [16] proposed cyclostationary models for describing noise in SISO NBPLC systems where, in the latter, a characterization in the frequency-domain is given in addition to the time-domain. The characterization of the noise in the frequency domain is important to study the performance of OFDM. When an extension to MIMO NBPLC is considered, the noise model should also include the potential correlation between the different phases. This correlation in broadband PLC was analyzed in [17], [18]. The authors in [19], [20] studied the effect of noise correlation on channel capacity improvement. Yet, to the best knowledge of the authors, [4] is the only work that provided a model for cyclostationary correlated noise of a MIMO NBPLC. In this model, white noise spectrum is injected through multiple inputs to a frequency shift (FRESH) filter to generate noise samples at multiple outputs that are compatible with experimental noise measurements.

The authors of [4] generalized the FRESH filter architecture to a bank of finite-impulse-response filters for the generation of cyclostationary correlated noise in MIMO systems. They demonstrated that the corresponding results are compatible with experimental noise measurements conducted in the laboratory over a low voltage (LV) power line. Their performance metric is defined in terms of normalized mean-square-error (NMSE) between the cyclic auto/cross correlation of the measurements and the model.

III. SYSTEM MODEL

Figure 1 depicts the block diagram of the complex equivalent baseband model of the MIMO-based OFDM system

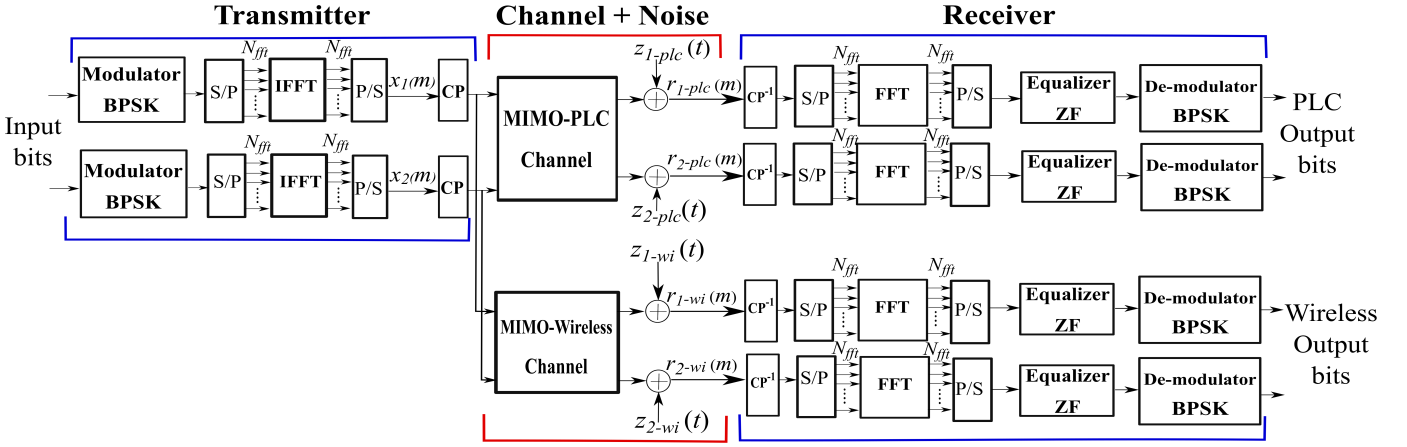


Fig. 1. Block diagram of the system with parallel MIMO-OFDM NBPLC and MIMO-OFDM Wireless links with BPSK modulation

with wireless and NBPLC links. The model in the figure was implemented in our simulations to compare the performance achieved on the two independent links for the same transmitted data sequence in one cycle of the cyclostationary noise. The performance achieved on the two links was used for implementing the proposed MIMO-OFDM WiNPLC system that will be described in Sec. IV. In the system of Fig. 1, two non-identical and parallel streams of bits are randomly generated and mapped using Gray encoding onto the constellation points. After the modulator, there is a serial-to-parallel (S/P) converter block whose role is that of splitting the high data rate stream into N_{fft} lower data rate parallel streams that are applied at the input of the inverse fast Fourier transform (IFFT) block. The N_{fft} samples at the output are applied at the input ports of both the two MIMO channels. To cancel the effect of ISI, a cyclic prefix (CP) is inserted between successive OFDM symbols that consists of N_{CP} samples, such that the length of CP is at least equal to the length of the channel impulse response measured in sampling intervals. Under this condition, the linear convolution of the input sequence transmitted over the channel is converted to a circular convolution. The two streams of samples are transmitted through 2×2 MIMO channels. In this system, we have two independent wireless and NBPLC MIMO channels. MIMO transmission in NBPLC consists of two phases while MIMO transmission in wireless refers to two links subject to frequency-flat Rayleigh fading. The cyclostationary noise is added to the signal at the output of the MIMO NBPLC channel while AWGN is added at the output of the MIMO Wireless channel. At each receiver, after the removal of the CP, the samples are first passed to a serial-to-parallel (S/P) converter and then sent to the FFT block. The N_{fft} samples at the output of the FFT are equalized using a zero forcing (ZF) equalizer in both links and, finally, the data is decoded.

A. Transmitter

Let $a_0(p), a_1(p), \dots, a_{N_{fft}-1}(p)$ be the block of transmitted symbols at the input of the IFFT at discrete-time p , where $a_k(p)$ is the symbol transmitted on the k th sub-carrier. In the

following, to simplify notation, the dependence on p will be omitted. After taking the N -point IFFT, the expression of the transmitted sample as:

$$x(m) = \frac{1}{\sqrt{N_{fft}}} \sum_{k=0}^{N_{fft}-1} a_k e^{j2\pi km/N_{fft}}, \quad m = 0, 1, \dots, N_{fft} - 1, \quad (1)$$

Considering the insertion of a CP of length N_{CP} , the m th transmitted sample is written as

$$\tilde{x}(m) = \begin{cases} x(N_{fft} + m), & m = -N_{CP}, \dots, -1, \\ x(m), & m = 0, \dots, N_{fft} - 1. \end{cases}$$

Here, we consider a system where two parallel streams of data are transmitted over the MIMO wireless link and two other over the MIMO NBPLC link as shown in Fig. 1.

The OFDM signal is generated by applying IFFT to $N_{fft} = 256$ points on the complex-valued signals produced at the output of the constellation mapper. A CP with $N_{CP} = 64$ symbols is added to the beginning of each OFDM symbol. Consequently, each stream consists of slots each with a length of 320 symbols.

B. Channel and Noise

1) *MIMO NBPLC Link*: Channel measurements from [11] are considered. Measurements were conducted in the laboratory over a LV power line in the range of frequencies between 0 and 200 kHz with inter-carrier spacing equal to 1.5625 kHz. Noise is generated by the FRESH filter that is proposed in [4]. The sampling frequency used is 400 kHz, which corresponds to the sampling frequency of CENELEC-A and CENELEC-B based on the IEEE 1901.2 standard. In our system, we have $K = 19$ branches for shifting the input signals in the FRESH filter and, for each branch, we have four filter coefficients $h_{11}, h_{12}, h_{21}, h_{22}$ that are generated based on real NBPLC noise measurements in the laboratory. Each filter coefficient is a vector with length equal to 50 which corresponds to the number of taps per branch. In Fig. 2, four noise cycles are depicted. This noise is cyclostationary with a periodicity of

half the AC cycle. With a sampling frequency of 400 kHz and AC cycle equal to 62.5 Hz, we have 3200 samples per cycle. Based on IEEE 1901.2 standard, each OFDM symbol consists of $N_{fft} = 256$ data samples and $N_{CP} = 64$ cyclic prefix samples. Consequently, each noise cycle coincides with 10 transmitted OFDM symbols.

2) *MIMO Wireless Link*: Similar to [11], each wireless link in the assumed 2×2 MIMO wireless system is assumed to undergo Rayleigh flat fading. No correlation is considered among the channel coefficients. The noise is assumed to be AWGN.

C. Receiver

After removing the CP and after the FFT, the received signal can be represented as follows

$$\begin{bmatrix} \mathbf{y}_1 \\ \mathbf{y}_2 \end{bmatrix} = \begin{bmatrix} H_{11} & H_{12} \\ H_{21} & H_{22} \end{bmatrix} \begin{bmatrix} \tilde{\mathbf{x}}_1 \\ \tilde{\mathbf{x}}_2 \end{bmatrix} + \begin{bmatrix} z_1 \\ z_2 \end{bmatrix}, \quad (2)$$

where $H_{j,i}$ is the coefficient of the channel matrix between the i th transmit antenna and the j th receive antenna and $z_{j,i}$ is noise vector.

IV. HYBRID WINPLC

Figure 3 shows three possible configurations of a hybrid system where a switch is implemented according to the strategies proposed in Sec. VI. The switching strategies are proposed after comparing the performance of the wireless and NBPLC links using the system shown in Fig. 1.

Figure 3a is the most practical from the hardware implementation point of view. Since we select by switching and not by combining, we can implement separate modems for the wireless and NBPLC link. The main benefit of the independent transmission design is that there is no need to develop a new modem for hybrid WinPLC, *i.e.*, we can simply use two of the shelf modems for wireless and NBPLC. However, the drawback is that the channel decoding will not benefit from the diversity of the hybrid system.

Figures 3b and 3c are designed assuming hybrid transmitters and receivers. The latter is proposed based on the fact that the noise in NBPLC is cyclostationary and we can predict its behaviour at the transmitter side. Therefore, the switching strategies at the transmitter side could be adjusted based on the average SNR in each cycle and perfect knowledge of the

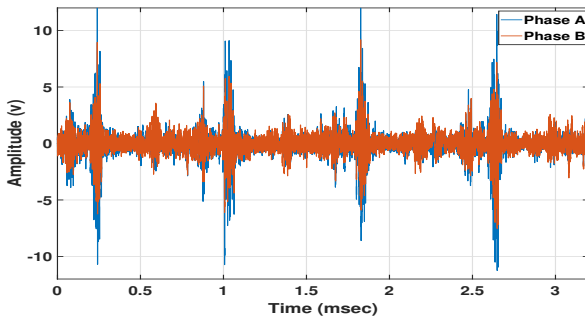


Fig. 2. Four cycles of cyclostationary noise generated by 2×2 MIMO FRESH filter for NBPLC.

NBPLC noise at the transmitter. Switching at the transmitter side in Fig. 3c has one more important advantage than the second configuration with single transmitter for parallel transmission and switching at receiver side. The advantage is that we can save transmitted power. In particular, when transmitting on NBPLC, the wireless link will not be active and, therefore, we save power. The same observation holds for NBPLC when we transmit over the wireless link. The authors in [21] analyzed transmitter switching versus receiver switching. They showed that switching at the transmitter side will save half of the power on average, which is reflected in a 3 dB SNR gain in the BER curves. Of course, switching at the transmitter side has the drawback of feedback overhead. However, in our system, the overhead is very small and it happens only at the beginning of the transmission.

In this work, we adopted the configuration in 3a, which is based on separate transmitters and receivers for the wireless and NBPLC links.

V. CYCLOSTATIONARY NOISE CLASSIFICATION

As mentioned in Subsection III-B1, the noise in our system is cyclostationary and in each period we have 3200 samples. We divide each noise period into 10 slots, therefore, each slot has 320 samples and could be considered as the noise added to one OFDM symbol. These noise samples are synthesized for N_{cycle} cycles of two phases over the power lines. In order to mitigate the effects of cyclostationary correlated impulsive noise, we have analyzed the features of noise samples.

As it can be seen in Fig. 2, in each noise period, of 8 ms, there are distinct regions with specific characteristics that are repeated in other cycles. Our goal is to detect these regions based on changes in statistics of the samples. Each region

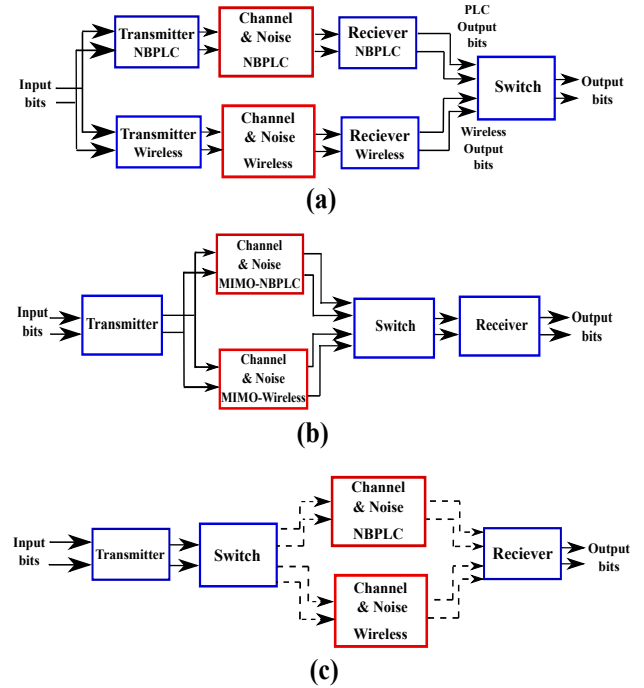


Fig. 3. Block diagram of the WinPLC system by switching between MIMO NBPLC and MIMO Wireless links for BPSK modulation

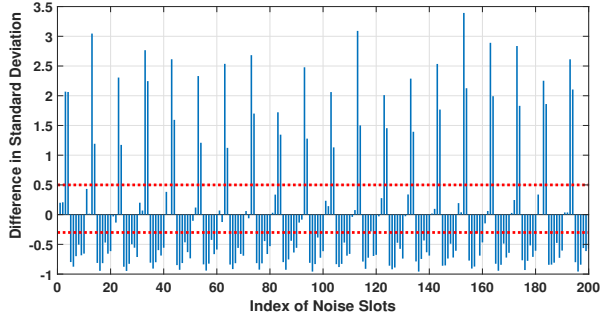


Fig. 4. Classification of noise for phase 1 based on difference between average and individual standard deviation of noise slots.

is considered as a separate class. Then, all the samples from N_{cycle} cycles that belong to a specific class are collected to analyze the behavior of each class. The classification algorithm used in our system consists of the following steps described in Algorithm 1:

- Step 1: Divide the noise samples to N_{slot} slots.
- Step 2: Evaluate $\sigma_{slot}(l)$, the standard deviation (SD) of each noise slot which consists of 320 samples.
- Step 3: Evaluate $\bar{\sigma}_{slot}(l)$, the standard deviation over all noise slots from the previous step.
- Step 4: Compute $diff_{slot}$, the difference between the standard deviation of each single slot and the average standard deviation of all slots.
- Step 5: Classify noise slots based on thresholds th_1 and th_2 .

Figure 4 demonstrates the performance of Step 4 and Step 5 in this Algorithm. The two thresholds are chosen empirically in such a way that for all periods the same noise slots are allocated to a certain class. Figure 5 shows that the noise classification in each cycle leads to allocating the last six slots of noise to class 1, the first two slots to class 2, and the remaining slots to class 3. After assigning each noise slot to a specific class as shown in Fig. 5, we collect all noise samples from N_{cycle} cycles which belong to that class. Figure 6 shows the histograms of the noise samples of each class and a red curve associated with the normal distribution that have been obtained by using the estimated mean and variance from the samples shown in the histograms.

The graphs reported in Fig. 6 demonstrate that noise samples generated by the FRESH model, and based on real

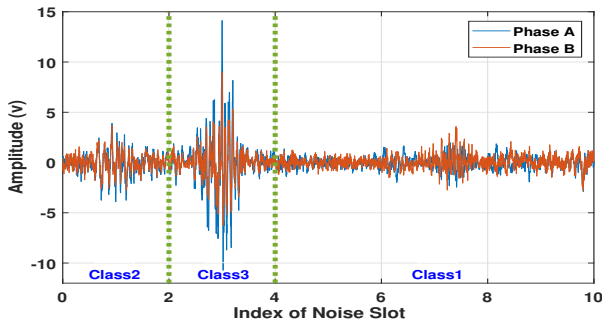


Fig. 5. Classification of noise slots in each cycle.

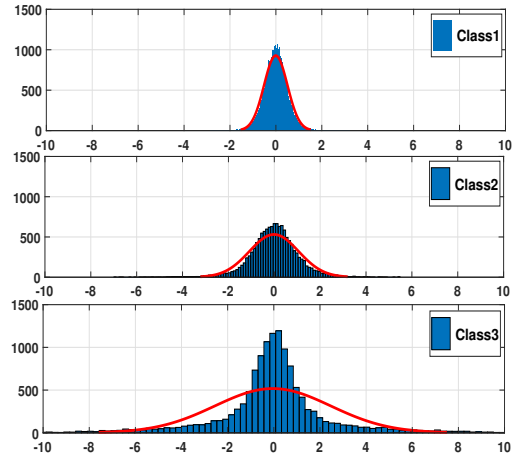


Fig. 6. Distribution of noise samples in each class

Algorithm 1 Cyclostationary Noise Classification

Inputs: Vector of cyclostationary noise \mathbf{z}_i , number of cycles N_{cycle} , thresholds th_1 and th_2 .

Initialization: Start with noise samples on phase 1, set $N_{slot} = 10N_{cycle}$, set $th_1 = -0.3$ and $th_2 = 0.5$.

- 1: **for** $l = 1, \dots, N_{slot}$ **do**
 - 2: $\mathbf{z}_{slot}(l) = \mathbf{z}(t)$, $t = 320(l - 1) + 1, \dots, 320l$
 - 3: $\sigma_{slot}(l) = \sigma_{\mathbf{z}_{slot}}(l)$
 - 4: **end for**
 - 5: $\bar{\sigma}_{slot}(l) = \frac{1}{N_{slot}} \sum_{l=1}^{N_{slot}} \sigma_{slot}(l)$
 - 6: **for** $l = 1, \dots, N_{slot}$ **do**
 - 7: $diff_{slot}(l) = \bar{\sigma}_{slot}(l) - \sigma_{\mathbf{z}_{slot}}(l)$
 - 8: $\begin{cases} \text{if } diff_{slot}(l) \leq th_1 & \rightarrow indx_{Class1} = l \\ \text{if } th_1 < diff_{slot}(l) < th_2 & \rightarrow indx_{Class2} = l \\ \text{if } th_2 \leq diff_{slot}(l) & \rightarrow indx_{Class3} = l \end{cases}$
 - 9: **end for**
 - 10: Record the index of noise slots associated with each class
 - 11: Use the same indexes for classifying the noise slots of phase 2
-

measurements, are equivalent to two Gaussian noise processes and one Middleton noise process, which correspond to the noise slots belonging to class1, class2, and class3, respectively. Consequently, each class has a certain level of SNR and BER. We assume that we have perfect knowledge of SNR of each class at the receiver side. Estimation of SNR is left to further investigations. In the following section we use Average SNR which is the average SNR associated with the three classes in one period.

VI. SIMULATION RESULTS AND ANALYSIS

In this section, simulation results for the SISO system are shown in Fig. 7 in terms of BER versus Average SNR

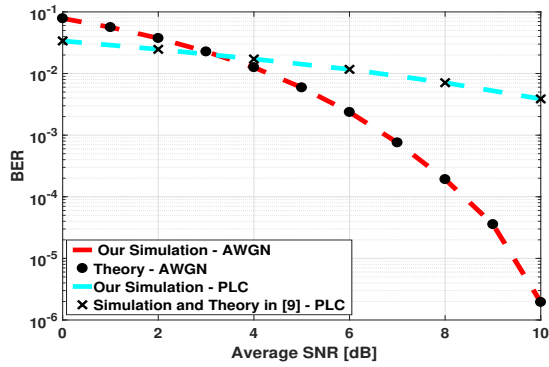


Fig. 7. Comparison between simulated and theoretical SISO-OFDM system over NBPLC and Wireless links in terms of BER versus Average SNR.

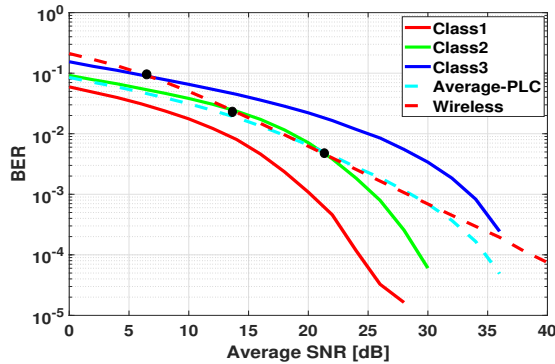


Fig. 8. Comparison between different classes of received data over NBPLC and data received through Wireless link in terms of BER vs average SNR [dB]

of all three classes in one cycle. We assume SISO-OFDM wireless and SISO-OFDM NBPLC links and the noises are AWGN and cyclostationary synthesized by the FRESH filter, respectively. For the case of SISO-OFDM NBPLC, the BER of our simulation is compared with that reported in Fig. 8 of [11], which provides both theoretical and simulation results. Figure 7 confirms that the result of our simulation for 1×1 SISO are in agreement with those available in the literature.

Next, simulations are run for 2×2 MIMO and achieve higher data rate. The simulated MIMO system is shown in Fig. 1 and described in Sec. III. The performance of this system, in terms of BER, is shown in Fig. 8 for different classes of noise. Figure 7 shows that the SISO-OFDM wireless link has better performance than the SISO-OFDM NBPLC at higher SNR. On the other hand, based on the noise analysis in Sec. V, in the presence of cyclostationary noise, NBPLC has periodic behaviour which is not uniform in each period according to the three classes. This classification enables a more precise comparison between MIMO wireless and MIMO NBPLC for each transmitted OFDM symbol. Figure 8 shows that when transmitting data under class1 noise in NBPLC, the BER of NBPLC is much lower than that of the wireless link for all SNRs. However, class2 and class3 noises are competitive with the wireless performance. This motivated us to consider a hybrid system by switching between wireless

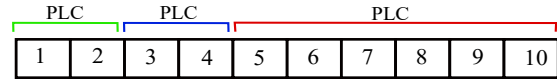


Fig. 9. Allocation of OFDM symbols to MIMO wireless and MIMO NBPLC in hybrid WinPLC in 1 period for $0 \text{ dB} < \text{average SNR} \leq 6 \text{ dB}$ with BPSK modulation

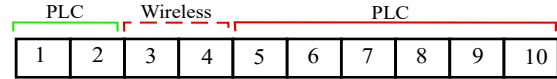


Fig. 10. Allocation of OFDM symbols to MIMO wireless and MIMO NBPLC in hybrid WinPLC in 1 period for $6 \text{ dB} < \text{average SNR} \leq 13 \text{ dB}$ and $21 \text{ dB} < \text{SNR}$ with BPSK modulation

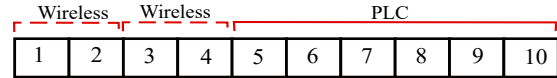


Fig. 11. Allocation of OFDM symbols to MIMO wireless and MIMO NBPLC in hybrid WinPLC in 1 period for $13 \text{ dB} < \text{average SNR} \leq 21 \text{ dB}$ with BPSK modulation

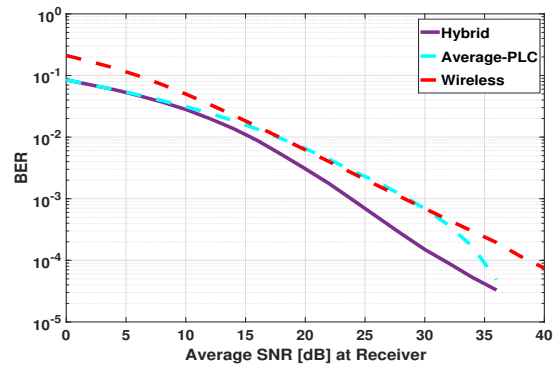


Fig. 12. Comparison of the performance between hybrid WinPLC, NBPLC, and Wireless in terms of BER vs average SNR for 2×2 MIMO-OFDM systems with BPSK modulation

and NBPLC. Figures 9, 10, and 11 clarify our switching strategies based on BER for different SNR levels obtained from Fig. 8. According to Fig. 8, the BER of NBPLC is always better than that of wireless for class1 noise, which coincides with the last 6 OFDM symbols in each period. For the first two OFDM symbols, the performance of wireless and class 2 of NBPLC are competitive. Similarly, for the third and the fourth OFDM symbols, wireless and class 3 of NBPLC must be compared. Figure 12 demonstrates the performance enhancement achieved by a hybrid MIMO-OFDM WinBPLC over a single MIMO-OFDM wireless and single MIMO-OFDM NBPLC links. As mentioned in Sec. IV, if we use switching at the transmitter side, we can save power and this saving depends on the average SNR. The reason is that switching strategies and transmission of different portions of data through wireless or NBPLC is based on average SNR. These switching strategies are valid while the average SNR at the receiver of NBPLC is equal to the SNR at the wireless receiver. However, there is also a possibility to have higher or lower average SNR at the wireless receiver, which needs to be studied in details and is left to future work.

VII. CONCLUSION AND FUTURE WORK

In this work, we have proposed an algorithm to classify the noise in a NBPLC system to three different classes based on its statistical characteristics. The analysis of the distribution of the noise samples reveals that cyclostationary noise in NBPLC is not uniform in each period and two classes have Gaussian behaviour while the third one is more impulsive. Next, we evaluated the performance of each class and compared the results for independent transmission of the same data over MIMO-OFDM wireless and MIMO-OFDM NBPLC systems. Simulation results show that the wireless link has lower BER for higher levels of SNR. However, the BER corresponding to data transmitted in presence of noise class1 is better than BER of the wireless link for all SNRs. Keeping this fact in mind, we have designed a hybrid system based on switching between the wireless and NBPLC links. The resulting system is the hybrid MIMO-OFDM WiNPLC system. For all levels of SNRs, the last 6 OFDM symbols in a period are transmitted through NBPLC. There is switching between wireless and NBPLC for the first 4 OFDM symbols. The different behavior of wireless and PLC as a function of average SNR is due to different statistics of the noise. The proposed hybrid system takes advantage of the independence of the noise and of the channel characteristics of the wireless and powerline links to improve the transmission reliability in smart grids. Performance of the hybrid system is better than wireless and near to the performance of NBPLC with the lowest level of noise. This hybrid system gave us the opportunity to ignore the harsh impulsive noise in NBPLC, which has a high impact on the performance of NBPLC. That is the reason for the gap between average-PLC and hybrid system for higher SNR. An important feature of our approach is that switching is done using only the average SNR of the three classes in each period, and not the SNR per sub-channel or per OFDM symbol. This aspect is interesting from a practical point of view since it has a very low complexity.

In future work, we plan to investigate in four directions. First, estimate the received SNR of each class precisely. Second, to analyze situations when the average SNR at the receiver of the wireless link is either less or greater than the average SNR at the NBPLC receiver. Then, adapt the switching strategies for these two cases. Our third future direction is to use adaptive modulation for different classes of the noise. Finally, we plan to compare the performance of adaptive NBPLC with that of wireless transmission and investigate the most suitable condition for switching between them and obtain optimized performance by adaptive hybrid MIMO-OFDM WiNPLC.

REFERENCES

- [1] L. Lampe, A. M. Tonello, and T. G. Swart, *Power Line Communications: Principles, Standards and Applications from Multimedia to Smart Grid*. Wiley Publishing, 2nd ed., 2016.
- [2] C. Cano, A. Pittolo, D. Malone, L. Lampe, A. M. Tonello, and A. G. Dabak, "State of the art in power line communications: From the applications to the medium," *IEEE Journal on Selected Areas in Communications*, vol. 34, pp. 1935–1952, July 2016.
- [3] M. Nassar, J. Lin, Y. Mortazavi, A. Dabak, I. H. Kim, and B. Evans, "Local utility power line communications in the 3 – 500 khz band: Channel impairments, noise, and standards," vol. 29, pp. 116–127, Sept 2012.
- [4] M. Elgenedy, M. Sayed, and N. Al-Dhahir, "A frequency-shift-filtering approach to cyclostationary noise modeling in mimo nb-plc," in *2016 IEEE Global Conference on Signal and Information Processing (GlobalSIP)*, pp. 881–885, Dec 2016.
- [5] M. Nassar, A. Dabak, I. H. Kim, T. Pande, and B. L. Evans, "Cyclostationary noise modeling in narrowband powerline communication for smart grid applications," in *IEEE International Conference on*, pp. 3089–3092, IEEE, 2012.
- [6] K. F. Nieman, J. Lin, M. Nassar, K. Waheed, and B. L. Evans, "Cyclic spectral analysis of power line noise in the 3-200 khz band," in *2013 IEEE 17th International Symposium on Power Line Communications and Its Applications*, pp. 315–320, March 2013.
- [7] M. Antoniali, F. Versolatto, and A. M. Tonello, "An experimental characterization of the plc noise at the source," *IEEE Transactions on Power Delivery*, vol. 31, pp. 1068–1075, June 2016.
- [8] M. Elgenedy, M. Sayed, M. Mokhtar, M. Abdallah, and N. Al-Dhahir, "Interference mitigation techniques for narrowband powerline smart grid communications," in *2015 IEEE International Conference on Smart Grid Communications (SmartGridComm)*, pp. 368–373, Nov 2015.
- [9] M. Elgenedy, M. Sayed, N. Al-Dhahir, and R. C. Chabaan, "Temporal-region-based cyclostationary noise mitigation for simo powerline communications," in *2018 IEEE International Conference on Communications (ICC)*, pp. 1–6, May 2018.
- [10] J. Sung and B. L. Evans, "Real-time testbed for diversity in powerline and wireless smart grid communications," in *IEEE ICC Workshops*, pp. 1–6, May 2018.
- [11] M. Sayed, G. Sebaali, B. L. Evans, and N. Al-Dhahir, "Efficient diversity technique for hybrid narrowband-powerline/wireless smart grid communications," in *Smart Grid Communications (SmartGridComm), 2015 IEEE International Conference on*, pp. 1–6, IEEE, 2015.
- [12] T. Oliveira, F. Andrade, A. Picorone, H. Latchman, S. Netto, and M. Ribeiro, "Characterization of hybrid communication channel in indoor scenario," *Journal of Communication and Information Systems*, vol. 31, no. 1, 2016.
- [13] L. d. M. B. A. Dib, V. Fernandes, M. de L. Filomeno, and M. V. Ribeiro, "Hybrid plc/wireless communication for smart grids and internet of things applications," *IEEE Internet of Things Journal*, vol. 5, pp. 655–667, April 2018.
- [14] J. Sung, M. Sayed, M. Elgenedy, B. L. Evans, N. Al-Dhahir, I. H. Kim, and K. Waheed, "Hybrid Powerline/Wireless Diversity for Smart Grid Communications: Design Challenges and Real-time Implementation," *arXiv e-prints*, p. arXiv:1808.04530, Aug 2018.
- [15] M. Sayed, T. A. Tsiftsis, and N. Al-Dhahir, "On the diversity of hybrid narrowband-plc/wireless communications for smart grids," *IEEE Trans. on Wire. Comm.*, vol. 16, pp. 4344–4360, July 2017.
- [16] M. Katayama, T. Yamazato, and H. Okada, "A mathematical model of noise in narrowband power line communication systems," *IEEE Journal on Selected Areas in Communications*, vol. 24, pp. 1267–1276, July 2006.
- [17] P. Pagani, R. Hashmat, A. Schwager, D. Schneider, and W. Baschlin, "European mimo plc field measurements: Noise analysis," in *IEEE Inter. Sym. on Power Line Comm.*, pp. 310–315, March 2012.
- [18] J. A. Cortes, J. A. Corchado, F. J. Canete, and L. Diez, "Analysis and exploitation of the noise correlation in mimo power line communications in the fm band," *IEEE Comm. Lett.*, vol. 22, pp. 566–569, March 2018.
- [19] D. Rende, A. Nayagam, K. Afkhamie, L. Yonge, R. Riva, D. Veronesi, F. Osnato, and P. Bisaglia, "Noise correlation and its effect on capacity of inhome mimo power line channels," in *IEEE Inter. Sym. on Power Line Comm. and Its Applications*, pp. 60–65, April 2011.
- [20] A. Pittolo, A. M. Tonello, and F. Versolatto, "Performance of mimo plc in measured channels affected by correlated noise," in *18th IEEE International Symposium on Power Line Communications and Its Applications*, pp. 261–265, March 2014.
- [21] M. Sayed, A. E. Shafie, M. Elgenedy, R. C. Chabaan, and N. Al-Dhahir, "Enhancing the reliability of two-way vehicle-to-grid communications," in *IEEE Intelligent Vehicles Symposium*, pp. 1922–1927, June 2017.